journal

J. Am. Ceram. Soc., 85 [3] 517–22 (2002)

Biomimetic Hydroxyapatite Coating on Metal Implants

Pamela Habibovic,[†] Florence Barrère,[†,‡] Clemens A. van Blitterswijk,[†,‡] Klaas de Groot,[†,§] and Pierre Layrolle[*,†,¶]

IsoTis NV, Professor Bronkhorstlaan 10, 3720 MB Bilthoven, The Netherlands

iBME, Twente University, The Netherlands

Biomaterial Research Group, Leiden University, The Netherlands

The combination of the high mechanical strength of metals with the osteoconductive properties of calcium phosphates make hydroxyapatite coatings on titanium implants widely used in orthopedic surgery. However, the most popular coating method, plasma spraying, exhibits some important drawbacks: the inability to cover porous implants and to incorporate biologically active agents, delamination, and particle release. The aim of this study was to elaborate a dense, strong, and thick calcium-phosphate coating on titanium and porous-tantalum implants using a two-step biomimetic procedure. In the first step, the implants were soaked in a solution that was 5 times more concentrated than regular simulated body fluid (SBF-A solution). A thin but uniform amorphous calcium-phosphate coating was deposited on the metal. Then, the implants were immersed in the SBF-B solution, which had a similar composition as the SBF-A solution, but with decreased contents of crystal growth inhibitors (i.e., Mg^{2+} and HCO_3^-). This resulted in the fast precipitation of a 30 μm thick crystalline calcium-phosphate coating. The pH of the SBF-B solution and the thickness of the crystalline coating layer were studied as a function of time. The Fourier transform infrared spectra and X-ray diffraction patterns showed that this new coating closely resembles bone mineral. Our biomimetic coating should facilitate rapid bone formation around the implant, reducing therewith the patient's recovery time after surgery.

I. Introduction

PLASMA sprayed coatings, mainly hydroxyapatite (HA), on titanium alloy (Ti6Al4V) prostheses have been widely used in orthopedic surgery to reconstruct hip and knee joints. Earlier investigations have shown that these coatings can successfully enhance clinical success to a <2% failure rate after 10 years.[1] Despite excellent clinical performances, the plasma-spray process is limited by intrinsic drawbacks. For instance, this line-of-sight process takes place at high temperatures. The process is, therefore, limited to thermally stable phases such as HA, and the incorporation of growth factors that stimulate bone healing is impossible. Moreover, this process cannot provide even coatings on porous metal surfaces.

Recently, other techniques have been studied to improve the quality of coatings, such as electrophoretic deposition,[2] sputter deposition,[3] and sol–gel.[4] Nevertheless, the deposition of apatite coatings from simulated body fluids (SBFs) offers the most promising alternative to plasma spraying and other coating methods. The biomimetic approach has four main advantages: (i) it is a low-temperature process applicable to any heat-sensitive substrate including polymers;[5] (ii) it forms bonelike apatite crystals having high bioactivity and good resorption characteristics;[6] (iii) it is evenly deposited on, or even into, porous or complex implant geometries;[7] and (iv) it can incorporate bone-growth-stimulating factors.

This biomimetic approach consists of soaking metal implants in simulated body fluids at a physiologic temperature and pH. Apatite coatings have successfully been formed by the immersion of chemically pretreated substrates such as glasses, metals, and polymers in metastable SBFs.[8–10] Although SBF mimics the inorganic composition, pH, and temperature of human blood plasma, it is unknown whether these conditions are optimal for a coating process. Indeed, a thin apatite layer has previously been obtained on pretreated substrates by using long immersion time (i.e., 7–14 days) with a daily refreshment of SBFs.[11–13] The difficulty results from the metastability of SBF. The process requires replenishment and a constant pH to maintain supersaturation for apatite crystal growth. As a result of the low solubility product of HA and the limited concentration range for the metastable phase, this operation is extremely difficult and might lead to local precipitation or uneven coatings. Such an intricate and long process can hardly be applicable in the coating prostheses industry.

This paper describes a new biomimetic route for coating titanium alloy and porous tantalum with uniform and thick HA layers in a few hours. Thereby, no chemical pretreatment of the substrate is needed. Our process takes advantage of the higher solubility of calcium phosphate in acidic conditions and its precipitation at a neutral pH. A weak gaseous acid, CO_2, is used to decrease the pH, allowing much higher ionic concentrations for SBFs. While CO_2 gas is naturally released from the solution, the pH and, therewith, saturation, are slowly and uniformly increased. Therefore, carbonate-containing HA crystals precipitate on the implants.

II. Experimental Procedure

(1) Materials

The biomimetic coatings were applied on two different materials: Ti6Al4V plates (20 mm × 20 mm × 1 mm; Smitfort Staal BV, Zwijndrecht, The Netherlands) and porous tantalum cylinders. The adhesion strength of the coating is dependent on the mechanical interlock of the biomimetic HA coating and the implant surface.[14,15] For optimal coating, an average surface roughness of 3.5 μm is required. This surface roughness on the Ti6Al4V plates was obtained via grit blasting, using corundum particles with a particle size of 595–841 μm under a pressure of 4 bar (Stratec Medical, Obendorf, Switzerland).

The porous tantalum implants were manufactured by chemical vapor infiltration of pure tantalum onto a highly porous vitreous

N. P. Padture—contributing editor

Manuscript No. 187738. Received April 30, 2001; approved October 26, 2001.
*Member, American Ceramic Society.
[†]IsoTis NV.
[‡]iBME, Twente University.
[§]Biomaterial Research Group, Leiden University.
[¶]Author to whom correspondence should be addressed (E-mail address: pierre.layrolle@isotis.com).

Table I. Inorganic Composition of Human Blood Plasma (HBP), Simulated Body Fluid (SBF), and Coating Solutions SBF-A and SBF-B

Component	Ion concentration (m*M*)							
	Na^+	K^+	Ca^{2+}	Mg^{2+}	Cl^-	HPO_4^{2-}	HCO_3^-	SO_4^{2-}
HBP	142.0	5.0	2.5	1.5	103.0	1.0	27.0	0.5
SBF	142.0	5.0	2.5	1.5	148.8	1.0	4.2	0.5
SBF-A	714.8		12.5	7.5	723.8	5.0	21.0	
SBF-B	704.2		12.5	1.5	711.8	5.0	10.5	

carbon skeleton (Implex Corp., Allendale, NJ). The porosity of the structure was ~75%, and the average size of the interconnected pores was 450 μm. Before coating, the implants were ultrasonically cleaned for 15 min in acetone, ethanol (70%), and demineralized water.

(2) Coating Solutions

The coating process consisted of two steps. In the first step, the heterogeneous nucleation of a thin and amorphous calcium phosphate layer on the metal surface was obtained. During the second step, the growth of a thick and crystallized apatite coating on the implants was favored because of the lower Mg^{2+} and HCO_3^- contents.

The SBF-A and SBF-B solutions (Table I) were prepared according to Kokubo's SBF solution,[16] excluding the TRIS-buffer, K^+ ions, and SO_4^{2-} ions. In the first-step solution, the SBF-A was 5 times more concentrated in NaCl, $MgCl_2 \cdot 6H_2O$, $CaCl_2 \cdot 2H_2O$, $Na_2HPO_4 \cdot 2H_2O$, and $NaHCO_3$ than Kokubo's SBF solution. The SBF-B solution had the same composition as the SBF-A solution but, as explained earlier, the contents of inhibitors of crystal growth (i.e., Mg^{2+} and HCO_3^- were lower (Table I)). All salts (reagent grade; Merck, Darmstadt, Germany) were precisely weighed (±0.01 g) and dissolved in demineralized water under a supply of CO_2 gas at a flow of 650 L/min for 20 min and stirring at a speed of 250 rounds per minute (rpm).

The pH evolution was studied as a function of time in coating the SBF-A and SBF-B solutions. As a reference, the pH development in time was studied in a solution containing NaCl at a concentration of 683 m*M* in demineralized water.

(3) Coating Process

All experiments were performed in a 7L bioreactor (Applikon Dependable Instruments, Schiedam, The Netherlands) (Fig. 1).

The implants were first soaked in a SBF-A solution for 24 h to seed the metal surface with calcium phosphate nuclei. During this process, the temperature was kept at 37°C and the solution was stirred at 250 rpm. To exchange CO_2 gas from the solution with air, a top aeration at a flow of 450 mL/min was performed. Moreover, air was added through the solution (500 mL/min flow) after the pH had reached a value of 7.1. At the end of the process, the coated samples were cleaned with demineralized water and dried in air overnight. Then, the implants were soaked for another 48 h in a SBF-B solution under crystal growth conditions. The temperature was maintained at 50°C and the stirring speed at 250 rpm. The same aeration system was used as described above. During this process, two samples were removed from the solution after 1, 2, 3, 4, 5, 6, 7, 8, 24, and 48 h. Finally, the coated samples were cleaned with demineralized water and dried in air overnight. At the end of both processes, the solutions were filtered through Whatman filter paper No. 5 (Whatman, Inc., Clifton, NJ). The precipitate was collected and dried at 50°C overnight.

(4) Chemical and Structural Characterization of the Coatings

All samples were first investigated macroscopically. After gold-sputtering, the coated samples were observed microscopically using an environmental scanning electronic microscope apparatus equipped with a field-emission gun (ESEM-FEG; Model XL-30, Philips, Eindhoven, The Netherlands) at an accelerating voltage of 10 keV, coupled with energy-dispersive X-ray analysis (EDAX) to check for any calcium-phosphate coating. The thickness of the coating was determined using an Eddy-current (electromagnetic) test method (Electrophysic Minitest 2100, Radiometer, Copenhagen, Denmark).[17] Both coating and precipitate were investigated by Fourier transform infrared spectroscopy (FTIR; Model Spectrum 1000, Perkin–Elmer Analytical Instruments, Norwalk, CT) and X-ray diffraction (XRD; Miniflex goniometer, Rigaku, Tokyo, Japan). X-rays were produced by a monochromatic source (Cu*K*α, λ = 1.54 Å, 30 kV, 15 mA). All the XRD patterns were recorded at the same conditions (scan range: $2\theta = 3.00°–60.00°$; scan speed: 2.00°/min; scan step: 0.02°). The crystallinity of the coating[18] and the calcium phosphate ratio[19] were determined. Both coatings and precipitate have similar FTIR spectra and XRD patterns. For convenience, analyses were performed on the precipitate.

III. Results

(1) pH Study

Comparing the pH curves versus time in the NaCl reference solution and the SBF-A and SBF-B solutions, it was observed that the initial pH of the NaCl reference was significantly lower (3.7) than the initial pH values of the SBF-A and SBF-B solutions (5.8 and 5.7, respectively). The end pH of the NaCl reference (6.6) after 24 h was lower as well (pH_{end} SBF-A = 8.3; pH_{end} SBF-B = 7.9). Moreover, the pH of the NaCl reference and SBF-A solution increased progressively from the beginning to the end of the process, while during the process in the SBF-B solution, a drop in the pH was observed.

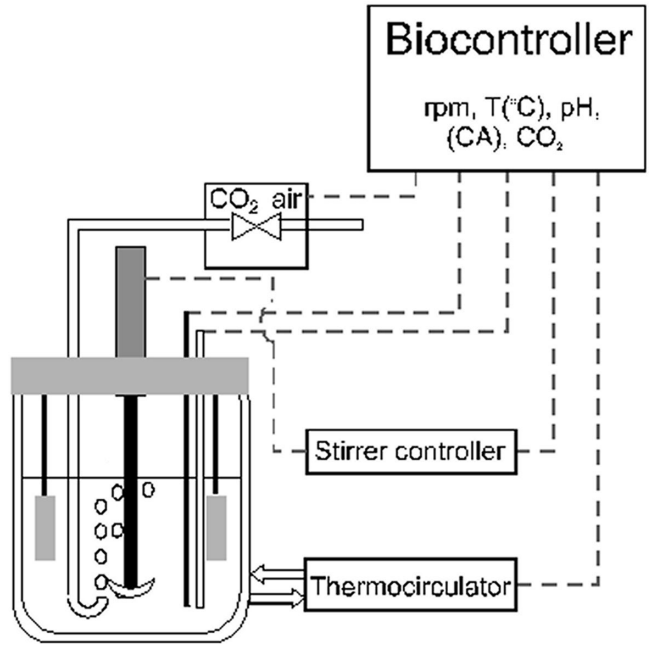

Fig. 1. Bioreactor for biomimetic coating of the metal implants.

(2) Coating Process

After 24 h of soaking in the SBF-A solution, the implants were covered with a calcium phosphate film with a thickness of ~3 μm. The ESEM photographs showed that this calcium phosphate layer was uniformly deposited on the Ti6Al4V surface (Fig. 2(a)). The coating was dense and consisted of globules. This thin coating exhibited some cracks, probably formed during the drying process of the coated samples. The EDAX spectrum (not shown) indicated calcium and phosphate peaks, with minute contents of magnesium and sodium. Small peaks of the Ti6Al4V substrate were also detected. The FTIR spectrum of the precipitate and coating (Fig. 3(a)) showed featureless phosphate and carbonate bands. Intense and broad bands assigned to oxygen-hydrogen stretching and bonding were observed at 3435 and 1642 cm^{-1}, respectively. Moreover, three bands at 868, 1432, and 1499 cm^{-1} corresponded to the CO_3 groups. Finally, the one-component bands at 560 and 1045 cm^{-1} showed the presence of PO_4. This FTIR spectrum is characteristic of carbonated amorphous calcium phosphate. The XRD pattern of the SBF-A precipitate (Fig. 4(a)) corroborates the FTIR results, showing only the halo characteristic of an amorphous phase.

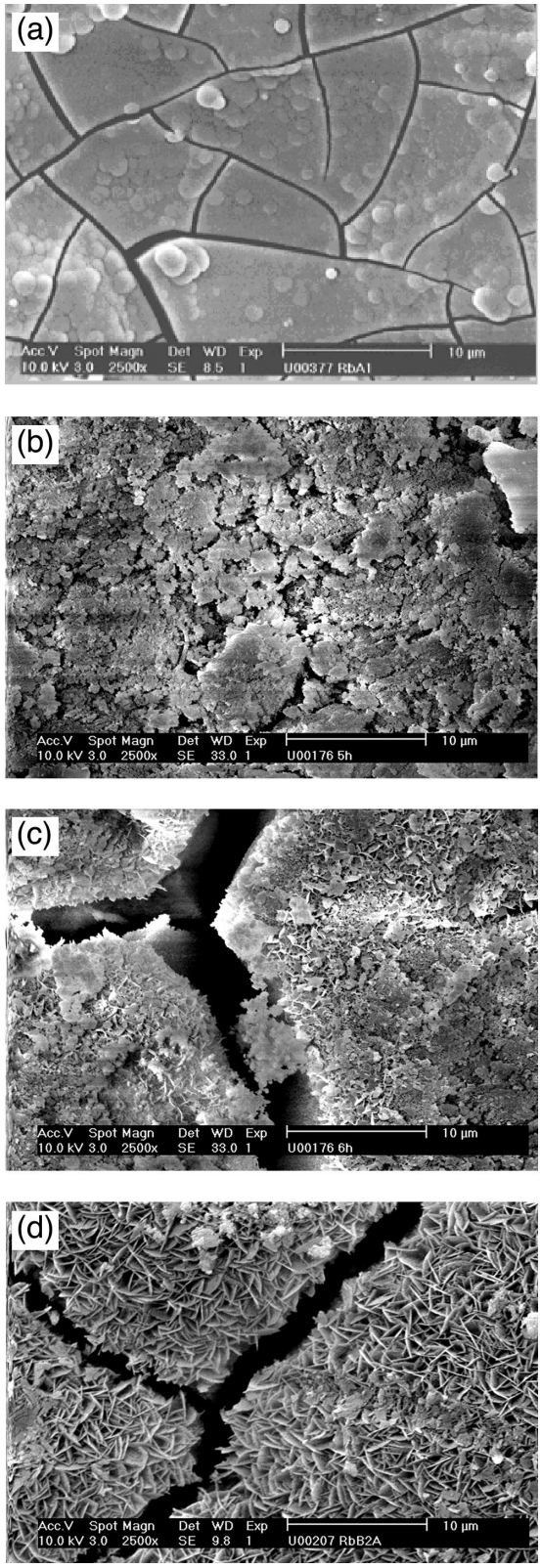

Fig. 2. ESEM photographs (magnification 2500×) of (a) SBF-A coating, (b) SBF-B coating after 5 h, (c) SBF-B coating after 6 h, and (d) SBF-B coating after 24 h on a Ti6Al4V plate.

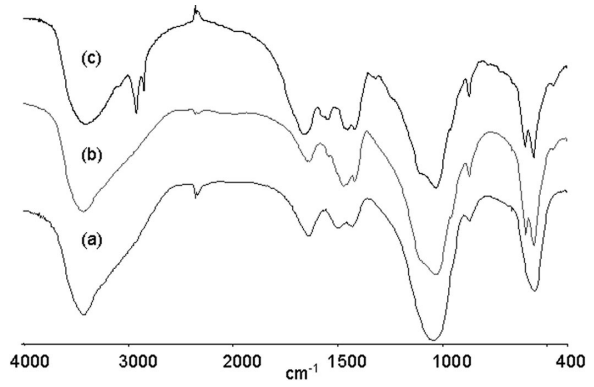

Fig. 3. Infrared spectra of (a) SBF-A coating, (b) SBF-B coating, and (c) bone.

The immersion process in the SBF-B solution was used to develop a second coating layer on the seeded Ti6Al4V surface resulting from the first coating process. During the immersion process in the SBF-B solution, the pH and coating thickness development were studied (Fig. 5). The pH of the solution at the beginning of the process stabilized at 5.7. During the first 4 h of the process, the pH increased progressively until a value of 6.2. Then, after 4 h, a drop of 0.4 pH units occurred. After this drop, the pH started increasing again, and reached a value of 8.2 after 24 h. The pH elaboration of the solution was followed until 48 h, and the final pH was 8.9.

During the first 4 h of the process, the solution remained clear, and the thickness of the second coating layer grew very slowly (i.e., ≤1.5 μm/h). During the drop in the pH, the precipitation occurred in the solution. After the pH drop, the coating thickness started increasing significantly with the rise in pH. Between 5 and 6 h of the immersion, the coating thickness grew to ~30 μm, after which it remained constant up to 48 h of soaking.

The ESEM photographs of the titanium implants after 5 and 6 h of immersion (Figs. 2(b) and (c)) show many differences. After 5 h, the metal was covered with loose calcium phosphate

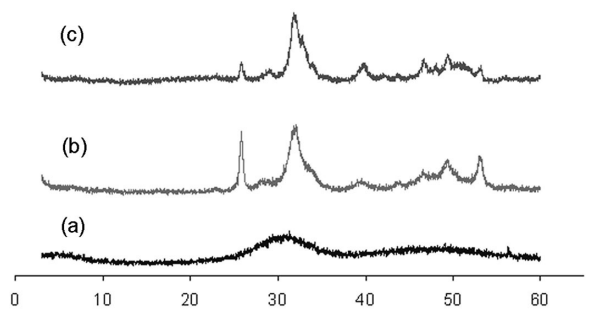

Fig. 4. XRD patterns of (a) SBF-A coating, (b) SBF-B coating, and (c) bone.

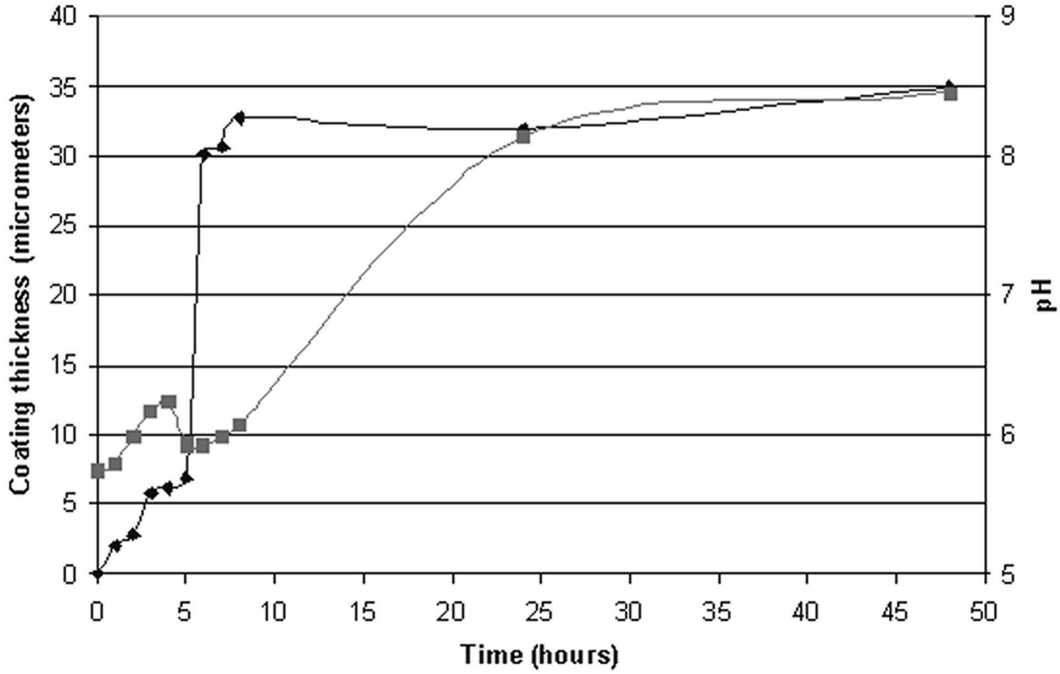

Fig. 5. (■) pH and (♦) coating thickness versus immersion time in SBF-B solution.

particles. The surface looked rough, without any visible crystals, and the thickness of the calcium phosphate layer was locally different. After 6 h of immersion, the coating thickness was 30 μm. In this case, the entire metal surface was homogeneously covered with a well-formed, bluish coating consisting of globules with some tiny crystals. The coating contained many wide cracks. After 24 h of soaking, the thickness of the coating did not change significantly in comparison to the coating after 6 h of soaking. However, the coating looked more homogeneous and denser (Fig. 2(d)), the cracks were much narrower, and the surface consisted of well-formed crystals 1–3 μm in size.

As explained earlier, the EDAX spectrum of the coating from the SBF-A solution showed high calcium and phosphate peaks, and lower magnesium, sodium, and titanium peaks. The EDAX spectrum of the coating after 5 h of soaking in the SBF-B solution showed lower calcium and phosphate peaks and a higher titanium peak, suggesting partial dissolution of the amorphous coating. The magnesium peak was also lower, indicating a difference in the amount of magnesium ions in the coating obtained from the SBF-A and SBF-B solutions. After 6 h of soaking in the SBF-B solution, an increase in phosphate and calcium peaks and a decrease in titanium peaks corroborated the growth of the coating. Finally, the EDAX spectrum of the coating after 24 h of soaking showed very high calcium and phosphate peaks, while the titanium peak was not visible anymore.

The ESEM photograph of the surface of porous tantalum cylinders after 24 h of immersion in SBF-B solution (Fig. 6(a)) indicates that the porous structure was homogeneously covered with a crystalline calcium-phosphate coating. On the cross-sectional surface (Fig. 6(b)), a coating was also visible on the inside of the implant. All pores were well-coated with a thick calcium phosphate layer.

The FTIR spectrum of the precipitate from the SBF-B solution, gathered between 400 and 4000 cm^{-1} (Fig. 3(b)), exhibited the characteristics of a carbonated apatite type A-B. The bands at 3435 and 1640 cm^{-1} corresponded to the oxygen-hydrogen groups. CO_3 group bands were observed at 1493, 1417, and 872 cm^{-1}, whereas bands at 1061, 599, and

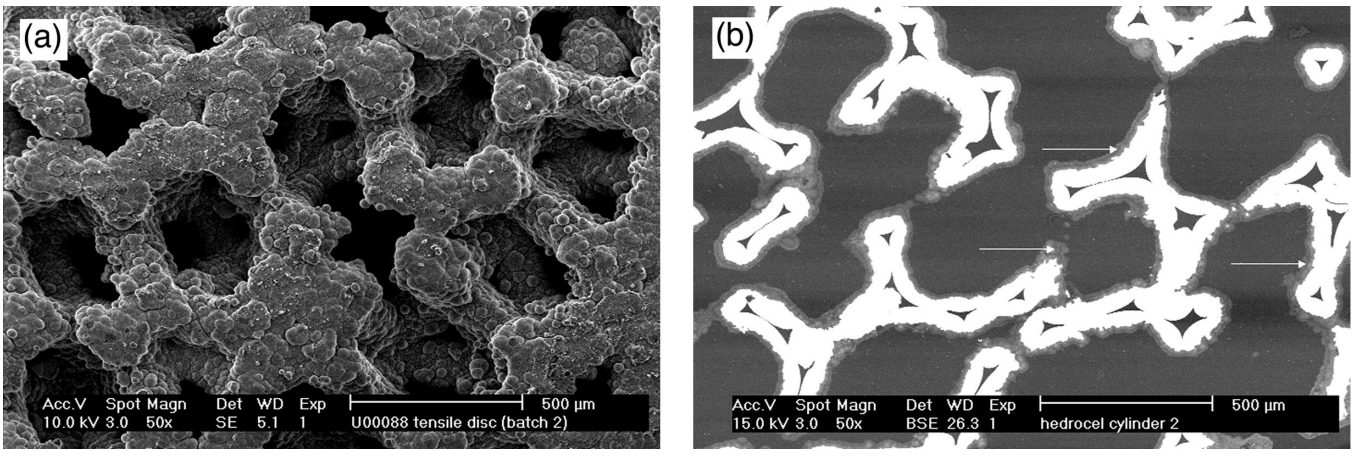

Fig. 6. ESEM photographs (magnification 50×) of (a) SBF-B coating on the surface and (b) cross section of porous tantalum cylinders; white arrows indicate the coating.

563 cm^{-1} were assigned to PO_4/HPO_4 groups. The XRD pattern exhibited broad diffraction lines (Fig. 4(b)). The position and intensities of these diffraction lines indicated an apatitic structure. The peak at $2\theta = 32.1°$ corresponded to the overlapping of (211), (112), (300), and (202) diffraction peaks. Moreover, the peak at $2\theta = 25.8°$, corresponding to the (002) diffraction plane, indicated that the SBF-B precipitate consisted of small apatitic crystals. The crystals had a size of 2–3 μm. The crystallinity of the precipitate was 75%, and its calcium phosphate ratio was 1.67.

Previously published results[20] showed that the final apatite coating is well-adhered to the Ti6Al4V substrate, and that no coating delamination or spalls were observed during the scratch test.

IV. Discussion

The results of the experiments show that highly-concentrated solutions can be obtained by the addition of the mildly acidic gas, CO_2. It is, namely, well-known that the solubility of calcium phosphate salts increases with the decrease of pH.[21] Dissolution of CO_2 gas results in a pH decrease caused by the formation of carbonic acid H_2CO_3 (reaction (1)), after which the acid immediately dissociates in the HCO_3^- and CO_3^{2-} species (reactions (2) and (3)).

$$CO_2 + H_2O \leftrightarrow H_2CO_3 \quad (1)$$

$$H_2CO_3 + H_2O \leftrightarrow HCO_3^- + H_3O^+ \quad (2)$$

$$HCO_3^- + H_2O \leftrightarrow CO_3^{2-} + H_3O^+ \quad (3)$$

When CO_2 gas gradually releases from the solutions, the pH slowly increases again. In the case of the NaCl reference, the pH increases progressively from the start to finish of the process, slowly approaching the pH of water (6.5). The presence of HCO_3^- and HPO_4^{2-} ions in SBF solutions, together with the CO_2 and HCO_3^- ions that are formed during the dissolution of CO_2 gas (reactions (2) and (3)), leads to the formation of a buffered solution. This might explain the fact that the initial pH values of the SBF-A and SBF-B solutions were higher than that of the NaCl reference. During the processes in the SBF-B solution, a drop in the pH was observed simultaneously with the start of precipitation in the solution. This drop of the pH may be explained by the start of the precipitation of the crystalline phase, according to reaction (4).

$$10Ca^{2+} + 6PO_4^{3-} + 2OH^- \leftrightarrow Ca_{10}(PO_4)_6(OH)_2 \quad (4)$$

Because of the decreased amount of OH^- ions in the solution, a pH drop was observed. After precipitation, CO_2 gas continued to release from the solution and, therefore, the pH increased progressively until the end of the process.

In the SBF-A solution, more HCO_3^- species were present in comparison with the SBF-B solution (Table I). Therefore, the buffering capacity of the CO_2/HCO_3^- couple was higher. This might explain a slightly higher initial pH and the absence of pH drop during the process in the SBF-A solution, in comparison with the process in the SBF-B solution.

Another factor that may influence the pH evolution during the coating process is the amount of the NaCl species, i.e., the ionic strength of the solution.[22] The rate of the CO_2 release from the solution is higher in the case of low ionic strength, followed by a higher pH increase. This causes an early and sudden precipitation in the solution. Consequently, the supersaturation of the solution is markedly lowered, and less ionic species' are available in the solution for the calcium phosphate nucleation on the substrate. Moreover, there is a relation between the calcium phosphate concentration and the pH at which precipitation occurs: the lower the concentration, the higher the precipitation pH.[21]

As was previously described, a 3 μm thick amorphous layer of carbonated calcium phosphate was obtained on the metal sample by immersion in the SBF-A solution. *In vivo* experiments performed by our group (unpublished results) showed that this amorphous coating was too thin to be able to enhance osteointegration of the implants. Moreover, earlier *in vitro* dissolution experiments[23] showed that, at both an acidic and neutral pH, amorphous carbonated calcium phosphate dissolves markedly faster than other calcium-phosphate coatings (i.e., octacalcium phosphate (OCP), carbonated apatite (CAp), and HA).

According to the literature and our experience, a coating that successfully enhances osteointegration of metal implants needs to be thick and crystallized enough to accommodate the bone healing process. Preliminary experiments were performed in order to grow a crystalline coating on a metal surface without immersion in the SBF-A solution. By immersing cleaned Ti6Al4V directly into the SBF-B solution, a loose and nonuniform layer was obtained, which shows the relevance of amorphous precoating. That is why our biomimetic coating consists of two steps.

Immersion of the implants in a SBF-A solution is necessary for seeding the metal surface with calcium phosphate nuclei. During this nucleation process, calcium phosphate seeds are precipitated in the solution and on the metal surface. Some of these nuclei can dissolve in the solution and some can expand in size. Homogeneous nucleation (precipitation) occurs spontaneously in the solution and can proceed if other seeds form in the meantime. Heterogeneous nucleation, on the other hand, takes place on the metal surface. Both, homogenous and heterogeneous nucleation are in competition during the process in the SBF-B solution. However, nuclei are energetically more stable on the seeded metal surface than in the solution. It is, therefore, essential to provide the metal surface with a thin and uniform primer calcium phosphate layer for subsequent growth of the final coating. The kinetics of the process in the SBF-A solution were reported in detail by Barrère *et al.*[24]

After reaching their critical size, seeds can start growing into crystals. The nucleation and growth kinetics of the crystal depend on the temperature, pH, composition, and saturation of the solution. Calcium and phosphate ions are responsible for the formation of the calcium phosphate layer on the metal surface, while magnesium and carbonate ions favor heterogeneous nucleation rather than crystal growth. As is given in Table I, the SBF-B solution has the same composition as the SBF-A solution, but the contents of Mg^{2+} and HCO_3^- ions are lower. Resulting from lower amounts of these so-called crystal growth inhibitors,[25–32] a crystalline apatite phase is formed and a drop in the pH is observed at the start of precipitation by immersion in the SBF-B solution. Moreover, a smaller amount of HCO_3^- ions, compared to the SBF-A solution, decreases the buffering capacity of the CO_2/HCO_3^- couple and, thereby, variations in the pH can be observed. With a lower amount of Mg^{2+} in the SBF-B solution, the calcium phosphate precipitation is accelerated, and the growing coat becomes more crystallized. Earlier research[33–36] proved that crystal growth from a supersaturated solution occurs quickly. This can explain the fact that, within 1 h, the coating thickness grows by 25 μm. Because of precipitation and crystal growth, the amount of calcium and phosphate in the solution decreases. One hour after the start of precipitation, the contents of the calcium and phosphate are too low for further growth. Between the end point of crystal growth and the end of the process, there is equilibrium between the amount of calcium and the amount of phosphate in the coating and in the solution. However, the coating might dissolve and reprecipitate onto surface, resulting in a more homogeneous and denser coating at the end of the process.

As mentioned previously, dense adherent film is formed because of the heterogeneous nucleation on the metal surface. However, it is very difficult to prevent loose precipitate in the solution from sticking to the metal surface. This means that both phenomena contribute to film growth, but to a different extent.

There is a difference in the calcium/phosphate ratio between natural calcified tissues (enamel, dentine, and bone) and the biomimetic coatings. The calcium/phosphate ratio of the natural calcified tissues is ~1.60, depending on many parameters such as age, sex, bone sites, etc.[37] The biomimetic coating has a calcium/

phosphate ratio of 1.67 ± 0.02, as determined after calcination at 1000°C by XRD and FTIR. In the case of the biomimetic coating, small amounts of magnesium and sodium can substitute for calcium in the HA lattice, lowering the calcium/phosphate ratio. However, carbonate is able to substitute for phosphate, which results in the transformation of HA into CAp, and increases the calcium/phosphate ratio. Because the second effect is much stronger, the overall effect is a higher calcium/phosphate ratio compared to bone.

The FTIR spectra (Fig. 3) and the XRD patterns (Fig. 4) show the similarities in composition and structure between our biomimetic coating and bone. An earlier report of an experiment with osteoclast-enriched mouse bone marrow cell cultures on different coatings[6] showed that numerous resorption lacunae, characteristic of osteoclastic resorption, were found on carbonated apatite after cell culture. In the case of OCP coating, no pits could be found. The obtained results indicated that biomimetic calcium-phosphate coatings are easily resorbed by osteoclasts *in vitro*. This phenomenon corresponds to full integration into the human body of biomimetically coated implants. On the contrary, conventional plasma-sprayed coatings may delaminate and release large sintered particles that are not easily degraded by cells.[38] The last results might indicate that our biomimetic coatings are markedly more bioactive than plasma-sprayed coatings. However, additional *in vivo* research is necessary to confirm these expectations.

V. Conclusion

The formation of thick and homogeneous calcium-phosphate coatings on Ti6Al4V implants and porous tantalum substrates is possible by using a biomimetic method consisting of two steps. By this method, the coating is produced within a few hours and without any chemical pretreatment. The first step of the process results in the formation of a thin amorphous coating, which finally leads to the fast precipitation of a 30 ± 10 μm thick dense calcium-phosphate coating in the second step of the process. The formation of this coating is strongly related to the Mg^{2+} content. The evolution of the pH during the coating process is dependent on the ionic strength of the solution (i.e., the amount of NaCl), and the amount of HCO_3^- ions, which, together with the present CO_2, buffer the solution. The final coating closely resembles bone mineral. The biomimetic coating applied on dense and porous orthopedic implants should enhance bone apposition and bone ingrowth, leading to the fast and stable osteointegration of prostheses.

References

[1]L. I. Havelin, L. B. Engesaeter, B. Espehaug, O. Furnes, S. A. Lie, and S. E. Vollset, "The Norwegian Arthroplasy Register, 11 Years and 73,000 Arthroplasties," *Acta Orthop. Scand.*, **71** [4] 337–53 (2000).

[2]P. Ducheyne, W. van Raemdonck, J. C. Heughebaert, and M. Heughebaert, "Structural Analysis of Hydroxyapatite Coatings on Titanium," *Biomaterials*, **7** [2] 97–103 (1986).

[3]J. L. Ong, L. C. Lucas, W. R. Lacefield, and E. D. Rigney, "Structure, Solubility and Bond Strength of Thin Calcium Phosphate Coatings Produced by Beam Sputter Deposition," *Biomaterials*, **13** [4] 249–54 (1992).

[4]B. Ben-Nissan, C. S. Chai, and K. A. Gross, "Effect of Solution Aging on Sol-Gel Hydroxyapatite Coatings," *Bioceramics*, **10**, 175–78 (1997).

[5]C. Du, P. Klasens, R. E. de Haan, J. Bezemer, F. Z. Cui, K. de Groot, and P. Layrolle, "Biomimetic Calcium Phosphate Coatings on PolyActive® 1000/70/30," *J. Biomed. Mater. Res.*, **59**, 535–46 (2002).

[6]S. Leeuwenburgh, P. Layrolle, F. Barrère, J. Schoonman, C. A. van Blitterswijk, and K. de Groot, "Osteoclastic Resorption of Biomimetic Calcium Phosphate Coatings *In Vitro*," *J. Biomed. Mater. Res.*, **56**, 208–15 (2001).

[7]P. Layrolle, C. van der Valk, R. Dalmeijer, C.A. van Blitterswijk, and K. de Groot, "Biomimetic Calcium Phosphate Coatings and Their Biological Performances," *Bioceramics*, **13**, 391–94 (2001).

[8]H. B. Wen, J. G. C. Wolke, J. R. de Wijn, F. Z. Cui, and K. de Groot, "Fast Precipitation of Calcium Phosphate Layers on Titanium Induced by Simple Chemical Treatment," *Biomaterials*, **18**, 1471–78 (1997).

[9]H. M. Kim, F. Miyaji, T. Kokubo, and T. Nakamura, "Preparation of Bioactive Ti and its Alloys via Simple Chemical Surface Treatment," *J. Biomed. Mater. Res.*, **32**, 409–17 (1996).

[10]S. Yamada, T. Nakamura, T. Kokubo, M. Oka, and T. Yamamura, "Osteoclastic Resorption of Apatite Formed on Apatite- and Wollastonite-Containing Glass-Ceramic by a Simulated Body Fluid," *J. Biomed. Mater. Res.*, **28**, 1357–63 (1994).

[11]P. Li, I. Kangasniemi, K. de Groot, and T. Kokubo, "Bonelike Hydroxyapatite, Induction by a Gel-Derived Titania on a Titanium Substrate," *J. Am. Ceram. Soc.*, **77**, 1307–12 (1994).

[12]T. Peltola, M. Patsi, H. Rahiala, I. Kangasniemi, and A. Yli-Urpo, "Calcium Phosphate Induction by Sol-Gel-Derived Titania Coatings on Titanium Substrates *In Vitro*," *J. Biomed. Mater. Res.*, **41**, 504–10 (1998).

[13]P. Li and P. Ducheyne, "Quasi-Biological Apatite Film Induced by Titanium in a Simulated Body Fluid," *J. Biomed. Mater. Res.*, **41**, 341–48 (1998).

[14]E. Leitao, M. A. Barbosa, and K. de Groot, "Influence of Substrate Material and Surface Finishing on the Morphology of the Calcium-Phosphate Coating," *J. Biomed. Mater. Res.*, **36**, 85–90 (1987).

[15]K. A. Thomas and S. D. Cook, "An Evaluation of Variables Influencing Implant Fixation by Direct Bone Apposition," *J. Biomed. Mater. Res.*, **19**, 875–901 (1985).

[16]T. Kokubo, H. Kushitani, S. Sakka, T. Kitsugi, and T. Yamamuro, "Solutions Able to Reproduce *In Vivo* Surface-Structure Changes in Bioactive Glass-Ceramics A-W3," *J. Biomed. Mater. Res.*, **24**, 721–34 (1990).

[17]"Standard Practice for Measuring Coating Thickness by Magnetic-Field or EDDY-Current (Electromagnetic) Test Methods," ASTM Designation E 376. *1996 Book of ASTM Standards*. American Society for Testing and Materials, West Conshohocken, PA.

[18]J. S. Flach, L. A. Shimp, C. A. van Blitterswijk, and K. de Groot, "A Calibrated Method for Crystallinity Determination of Hydroxylapatite Coatings"; in *Characterization and Performance of Calcium Phosphate Coatings for Implants*, ASTM Special Technical Publication 1196. Edited by E. Horowitz and J. E. Perr. American Society for Testing Materials, West Conshohocken, PA, 1994.

[19]"Determination Quantitative du Rapport Ca/P de Phosphates de Calcium"; Paper No. 94-066 in *Materiaux pour Implants Chirurgicaux*. Association Française de Normalisation (ANFOR), Paris, France, 1998.

[20]F. Barrère, P. Layrolle, C.A. van Blitterswijk, and K. de Groot, "Physical and Chemical Characteristics of Plasma-Sprayed and Biomimetic Apatite Coating," *Bioceramics*, **12**, 125–28 (1999).

[21]J. C. Elliot, *Structure and Chemistry of the Apatites and Other Calcium Orthophosphates*; p. 4. Elsevier, Amsterdam, The Netherlands, 1994.

[22]F. Barrère, P. Layrolle, C.A. van Blitterswijk, and K. de Groot, "Influence of NaCl and HCO_3 on the Biomimetic Ca-P Coating Process from SBFx5 Solution," *Biomaterials*, in press.

[23]F. Barrère, M. Stigter, P. Layrolle, C.A. van Blitterswijk, and K. de Groot, "*In Vitro* Dissolution of Various Calcium-Phosphates Coatings on Ti6Al4V," *Bioceramics*, **13**, 67–70 (2000).

[24]F. Barrère, P. Layrolle, C.A. van Blitterswijk, and K. de Groot, "Fast Formation of Biomimetic Ca-P Coatings on Ti6Al4V," *Mater. Res. Soc. Symp. Proc.*, **599**, 135–40 (2000).

[25]H. Newesely, "Changes in Crystal Types of Low Solubility Calcium Phosphates in Presence of Accompanying Ions," *Arch. Oral Biol.*, **6** [Special Supplement] 174–80 (1961).

[26]B. Tomazic, M. Tomson, and G. H. Nancollas, "Growth of Calcium Phosphates on Hydroxyapatite Crystals: The Effect of Magnesium," *Arch. Oral Biol.*, **20**, 803–808 (1975).

[27]M. H. Salimi, J. C. Heughbaert, and G. H. Nancollas, "Crystal Growth of Calcium Phosphates in the Presence of Magnesium Ions," *Langmuir*, **1**, 119–22 (1985).

[28]E. D. Eanes and S. L. Rattner, "The Effect of Magnesium on Apatite Formation in Seeded Supersaturated Solutions at pH = 7.4," *J. Dent. Res.*, **60** [9] 1719–23 (1980).

[29]A. L. Boskey and A. S. Posner, "Magnesium Stabilization of Amorphous Calcium Phosphate: A Kinetic Study," *Mater. Res. Bull.*, **9**, 907–16 (1974).

[30]G. H. Nancollas, B. Tomazic, and M. Tomson, "The Precipitation of Calcium Phosphate in the Presence of Magnesium," *Croatia Chemica Acta*, **48**, 431–38 (1976).

[31]N. S. Chikerur, M. S. Tung, and W. E. Brown, "A Mechanism for Incorporation of Carbonate into Apatite," *Calcif. Tissue Int.*, **32**, 55–62 (1980).

[32]B. N. Bachara and H. R. A. Fisher, "The Effect of Some Inhibitors on the Nucleation and Crystal Growth of Apatite," *Calcif. Tissue Res.*, **3**, 348–57 (1969).

[33]H. Füredi-Milhofer, L. Brecevic, and B. Purgaric, "Crystal Growth and Phase Transformation in the Precipitation of Calcium Phosphates," *Faraday Discuss. Chem. Soc.*, **61**, 184–90 (1976).

[34]P. Koutsoukos, Z. Amjad, M. B. Tomson, and G. H. Nancollas, "Crystallization of Calcium Phosphates: A Constant Composition Study," *J. Am. Chem. Soc.*, **102** [5] 1553–57 (1980).

[35]M. J. J. M. van Kemenade and P. L. de Bruyn, "A Kinetic Study of Precipitation from Supersaturated Calcium Phosphate Solutions," *J. Colloid Interface Sci.*, **118**, 564–85 (1987).

[36]G. T. Kohman, "Precipitation of Crystals from Solution"; pp. 152–62 in *The Art and Science of Growing Crystals*. Edited by J. Gilman. Wiley, London, U.K., 1963.

[37]R. LeGeros, *Calcium Phosphates in Oral Biology and Medicine*; pp. 109–27. Karger, Basel, Switzerland, 1991.

[38]J. D. de Bruijn, J. S. Flach, H. Leenders, J. van den Brink, and C.A. van Blitterswijk, "Degradation and Interface Characteristics of Plasma-Sprayed Coatings with Different Crystallinities," *Bioceramics*, **5**, 291–98 (1992). □